Molecular dynamics simulations of the interaction of glucose with imidazole in aqueous solution

Mo Chen, Yannick J. Bomble, Michael E. Himmel, John W. Brady

PII: S0008-6215(11)00592-1
DOI: 10.1016/j.carres.2011.12.008
Reference: CAR 6026

To appear in: *Carbohydrate Research*

Received Date: 15 June 2011
Revised Date: 22 November 2011
Accepted Date: 8 December 2011

Please cite this article as: Chen, M., Bomble, Y.J., Himmel, M.E., Brady, J.W., Molecular dynamics simulations of the interaction of glucose with imidazole in aqueous solution, *Carbohydrate Research* (2011), doi: 10.1016/j.carres.2011.12.008

Molecular dynamics simulations of the interaction of glucose with imidazole in aqueous solution

Mo Chen[†], Yannick J. Bomble[‡],

Michael E. Himmel[‡], and John W. Brady[*,†]

[†]Department of Food Science
Cornell University
Ithaca, NY 14853

[‡]Biosciences Center
National Renewable Energy Laboratory
1617 Cole Boulevard
Golden, CO 80401-3393

* Author to whom correspondence should be addressed; +1 (607) 255-2897; jwb7@cornell.edu

Abstract

Molecular dynamics simulations were carried out on a concentrated system of βD-glucopyranose and imidazole molecules in a periodic box of water at 298 K. The purpose of the simulations was to determine whether or not there was any tendency for these two solutes to associate in an aqueous environment, as has previously been observed for other planar functional groups from amino acid side chains, such as the indole group of tryptophan or the phenolic group of tyrosine. A weak stacking interaction between βD-glucopyranose, as a model for cellulose, and imidazole was indeed observed, with an energy of ~0.25 kcal/mol per pair, less than kT. Somewhat surprisingly, considerable imidazole self-association into small aggregates (dimers and trimers) was also observed, with binding energies of ~0.4 kcal/mol per pair, although still less than kT. Considerable non-stacked interactions between glucose and imidazole through hydrogen bonding were also found. These hydrogen bonds primarily involved the N3 atom of imidazole, because the N–H group of N1 was insufficiently polar to compete for water hydrogen bond partners.

Key Words: imidazole, molecular dynamics simulations, aqueous solution, water hydration, sugar binding

Introduction

Like many other sugars, glucose, with its multiple hydrogen-bonding hydroxyl groups, generally behaves as an osmolyte, strongly and favorably interacting with water. Glucose is drawn down into the bulk of the solution, away from interfaces and surfaces, including the surfaces of proteins, while it raises the surface tension of the solution. In a Hofmeister sense, it thus stabilizes protein conformations; however, by raising the chemical potential, it also favors their precipitation. Given this behavior, it would be expected that, in general, glucose would be preferentially excluded from the surfaces of proteins. However, there are a number of proteins that have been designed by evolution to specifically bind to sugars. Some of these proteins, such as lectins,[1-3] recognize and bind to sugars such as galactose or mannose. The sugar binding proteins,[4,5] such as arabinose-binding protein[6] or galactose-binding protein, are designed to bind to and transport sugars. Others, such as glycoside hydrolases like lysozyme, amylases, and cellulases, are enzymes that have carbohydrate substrates. Certain of the cellulases in particular not only contain a catalytic center designed to act on a carbohydrate substrate, but also possess a distinct binding domain designed to anchor the enzyme to its cellulose substrate via strong and specific binding.[7,8] The various cellulases are particularly interesting examples of sugar binding proteins because of their importance in biomass conversion efforts.[9]

In each of these classes of proteins, evolution has designed the sugar binding site so as to overcome the preference of sugars like glucose to fully hydrate and to avoid the surfaces of proteins. Since a number of crystal structures of proteins from each of these classes are now available, it is possible from surveying these structures to make some general statements about the types of interactions that favor sugar binding.[10] In particular, for sites that have an affinity for glucose, with its hydrophobic faces, a common feature is amino acid side chains that contain

planar functional groups like tryptophan, phenylalanine, tyrosine, and histidine. The flat faces of these rings are non-hydrogen bonding and thus so weakly hydrated as to be effectively hydrophobic. Presumably, their role in promoting the affinity for glucose is to match up their hydrophobic surfaces with the hydrophobic "tops" and "bottoms" of the beta anomer of glucose. Because of their extended surfaces, the indole groups of tryptophan side chains seem to be especially effective for this role, judging from the frequency of the occurrence of tryptophan in cellulase binding sites. However, histidine is also often found in such sites, in spite of its considerably smaller planar surface area. Figure 1 shows the binding site of one of the glucose-binding proteins,[11] indicating three such histidine residues in the ligand binding site. A conserved histidine residue also occurs in the active site tunnel of the Family 48 cellulase Cel48F from *Clostridium cellulolyticum*[12] (Figure 2), very close to the scissile bond of the substrate. Another histidine residue occurs near the entrance to the active site tunnel of the same protein (Figure 3), although that residue is not conserved across the Family 48 enzymes. It would be interesting to know whether there is any particular affinity for the imidazole group of histidine for glucose, the repeating monomer of the cellulose substrate for this and related enzymes; and, if so, if that interaction is mediated by hydrogen bonding, hydrophobic face-to-face stacking, or some other type of interaction.

Imidazole could potentially interact with glucose both as a planar hydrophobic surface and also as a hydrogen-bond acceptor to its N3 nitrogen atom (Figure 4). Recent studies of glucose interacting with the indole group of tryptophan found that the principal mode of interaction was by stacking the H1–H3–H5 hydrophobic triad of the glucose molecule against the flat, hydrophobic face of the indole rings.[13] The energy of this interaction was estimated to be approximately 1.2 kcal/mol, in agreement with experimental estimates. (Note that, due to a

computational error, the numbers reported in reference 13 are too small by a factor of 2.303.) [14] However, the relative orientations of the sugar ligand and three histidine imidazole groups in the crystallographic structure of GBP (Figure 1) suggest hydrogen-bonding interactions. In Cel48F, the His 36 residue not only is making direct interactions with the substrate, but probably more importantly, may be serving a catalytic role through its proximity to the catalytic acid Glu 55, due to its well-known ability to serve as a proton donor and acceptor as imidazolium. In its neutral, imidazole form, the charge distribution (as approximated in molecular mechanics simulations, see Figure 4)[15] can support strong hydrogen bonding as an acceptor to N3, but probably not to the N1-H group.

Here we report a molecular dynamics simulation of imidazole in an aqueous solution of glucose to examine what, if any, interactions take place between these two co-solutes, and between the neutral imidazole molecules themselves. Similar simulations have recently been used to study the interactions of glucose with the tryptophan residue of melittin from bee venom,[13] with the tyrosine residues of the cellulose binding module of the cellulase CBH I from *Trichoderma reesei*,[16] and with the purine, caffeine.[17] Understanding any interactions that take place between imidazole and glucose could help illuminate what role histidine side chains might be playing in the mechanisms of binding and hydrolysis in cellulases like the Cel48 family of proteins.

Procedures

Simulations were conducted in a manner similar to those previously reported for glucose interacting with melittin and caffeine.[13,17] The primary simulation box contained 30 imidazole molecules and 30 βD-glucopyranose molecules, with 555 TIP3P water molecules[18] in a cubic box with sides 29.6 Å in length. The TIP3P water model was chosen to facilitate comparisons with our previous studies of sugar binding to planar co-solutes.[13,16,17,19] This ratio produced concentrations of 3 molal in both the sugar and the imidazole. The initial coordinates for the system were generated by randomly placing each imidazole and glucose molecule into a previously equilibrated box of TIP3P water and removing any water molecules whose oxygen atom was closer than 2.4 Å to any solute heavy atom. Initial configurations were first minimized with 50 steps of steepest descent minimization to remove bad local contacts, after which the system was heated from 0 to 298 K over a 100 ps equilibration period. After equilibration, the simulations were run for an additional 15 ns in the canonical NVT ensemble using the CHARMM molecular mechanics program.[20,21]

The new CHARMM force field designed specifically for carbohydrates[22] was used for the glucose molecules, and the general CHARMM27 force field for the imidazole molecules.[15] The lengths of the covalent bonds involving hydrogen atoms were kept fixed using the SHAKE algorithm.[23,24] The Newtonian equations of motions were integrated using a time step of 1 fs. van der Waals interactions were smoothly truncated on an atom-by-atom basis using switching functions from 10.0 to 12.0 Å. Electrostatic interactions were treated using the particle-mesh Ewald method with a cutoff value of 12.0 Å.[25] The size of the box was adjusted to 29.6 Å to yield the density of water at 25°C. Atomic density analyses of the trajectory were displayed using the Visual Molecular Dynamics (VMD) graphics program.[26]

In an actual solution of glucose in water, the sugar would quickly undergo tautomerization, giving a 64:36% (β:α) ratio of the pyranoid anomers (the furanoid tautomers are present in only negligible proportions).[27] This anomerization was ignored in the present study because the primary interaction of interest is with the glucose monomers of cellulose, where each glucose is locked by the glycoside linkage into the beta configuration. Similarly, only the unprotonated imidazole form was present, representing a solution at neutral pH.

Results and discussion

Somewhat unexpectedly, given the very high solubility of imidazole in aqueous solution,[28] a weak tendency for imidazole to self-associate at this concentration was observed in the simulations, which is consistent with the results of a very recent study of imidazole in solution using both the AMBER point charge force field and a multipolar expansion model for the electrostatics.[29] Figure 5 displays the contoured density of imidazole molecules relative to a coordinate frame fixed with respect to a central imidazole, and averaged over all imidazoles in the simulation. As can be seen, there is a clear tendency for the molecules to pair in solution. Most of these interactions (~70%) are through perpendicular, or "T"-type, interactions, as seen in Figure 6a, with the N1–H bond of one molecule pointing toward the center of the second ring. A much smaller fraction of interactions, about 7.5%, take place by stacking against one another's hydrophobic faces (Figure 6b), in a manner similar to that seen for caffeine, which is known from osmotic experiments to form such aggregates.[17] Unlike the caffeine case, however, this tendency is much weaker for imidazole and no larger aggregates are seen. A third type of

imidazole pairing also has the two molecules perpendicular to one another, but with the N1–H bond of one molecule hydrogen bonded to the N3 atom of the second (Figure 6c); this chain-like type of interaction accounted for approximately 22.5% of the observed dimer pairs. Only one imidazole concentration was simulated in the present studies, but it has been suggested recently that system size could affect aggregation in some systems.[30] However, in previous simulations of similar systems which studied aggregation as a function of system size, we found no such effects.[31]

Liem et al also found associations of this type,[29] both with simulations using an AMBER point charge model, similar to the CHARMM model used here, and in calculations with electrostatic multipole moments. These workers only reported two types of dimers, the chain-like arrangement of Figure 6c and the face-to-face stacked arrangement of two of the molecules in Figure 6b. They did not report any of the T-type dimers of Figure 6a and the bottom pair of 6b. However, examination of their density distributions, shown for individual atoms types, reveals that significant pairing of this type occurred in their simulations as well. The proportion of stacked dimers compared to chain dimers in their simulations was much lower when using the multipole treatment of electrostatics.[29]

A weak affinity of glucose for imidazole was also observed in the present simulations. Figure 7 displays contours of high density for the H1, H3, and H5 protons of the glucose solutes relative to a reference frame fixed with respect to the imidazole ring, as well as separate density contours for the ring atoms and for H2 and H4. As can be seen, there is a high probability of a glucose molecule stacking against the flat faces of the imidazole solute, in a manner very similar to that previously seen for indole,[13,19] tyrosine,[16,19] and caffeine.[17] While this result might not be

completely unexpected given these previous studies, it was not obvious that glucose would stack in this manner given the much smaller flat surface area of the imidazole group. We also observed a strong preference for the β-D-glucopyranose molecules to be orientated with the H1–H3–H5 hydrophobic triad in van der Waals contact with the imidazole ring, and with the H2 and H4 protons pointing away, and with a very much lower probability for it to be oriented the other way around.

Using the same procedures previously employed for other systems,[13] the free energy of binding was estimated from the trajectory data. This was done by calculating a host–guest type equilibrium constant from the concentration of bound glucose, $K = \frac{[glucose \bullet imidazole]}{[glucose][imidazole]}$, which can be used to calculate the binding free energy $\Delta G = -RT \ln \frac{K}{K^o}$, with the standard state defined as the binding site volume occupied by bulk density glucose. The definition of the binding site is somewhat arbitrary to the extent that the choice of the density cutoff used to specify it is arbitrarily selected. However, the binding site is fairly well localized, so that the density falls off steeply with displacement away from the center of the ring. Thus, within a good range of cutoff values, the calculated energy does not change rapidly with the cutoff, allowing a qualitative estimate of the binding affinity that is not strongly dependent on the selection of cutoff, as is shown in Table 1 for a range of density cutoff values. As can be seen from the table, β-D-glucopyranose binds to the faces of the imidazole ring with an energy of approximately 0.5 kcal/mol, which is lower than the value found for the tryptophan residue in melittin,[13] but on the same order as computed from glucose–indole binding from potential of mean force calculations.[19] Note that these energies were computed from density data for the ring atoms (Figure 7) rather

than the proton positions. Imidazole–imidazole interactions, computed in the same fashion, are stronger, approximately 0.8 kcal/mol (Table 2).

Table 1. The binding energy for βD-glucopyranose pairing with imidazole calculated from the density data, as a function of the contour level selected to define the binding site.

contour level (times bulk density)	K_{eq}	calculated binding energy (kcal/mol)
2.2	2.38	-0.51
2.4	2.52	-0.55
2.6	2.68	-0.58
2.8	2.82	-0.61

Table 2. The binding energy for imidazole-imidazole pairing calculated from the density data, as a function of the contour level selected to define the binding site.

contour level (times bulk density)	K_{eq}	calculated binding energy (kcal/mol)
3.2	3.50	-0.74
3.4	3.64	-0.76
3.6	3.80	-0.79
3.8	3.95	-0.81

In addition to this hydrophobic stacking, however, glucose also interacts with solvated imidazole through hydrogen bonding. Figure 8 displays the density of glucose oxygen atoms around the imidazole ring. As can be seen, the density of the glucose ring oxygen atom O5 is only above and below the imidazole faces, resulting from stacking. The hydroxyl oxygen atoms, however, are arrayed around the ring in orientations that indicate hydrogen bonding. The density of these hydroxyl oxygen atoms forms a banana-shaped band arcing around the N3 position in particular, due to its strongly negative partial atomic charge, allowing it to make particularly strong interactions as a hydrogen bond acceptor. The presence of diffuse O6 oxygen atom density around the C–H positions of C2 and C4, but not C5, is harder to explain, but probably is the

incidental result of the topological constraint of the glucose molecule—if one of the O1–O4 hydroxyl groups is making a hydrogen bond to N3, the exocyclic hydroxyl group is more likely to be nearby due to topological constraints; this would explain why there is no such diffuse density around C5.

The radial distribution function $g_{NO}(r)$ for sugar hydroxyl oxygen atoms can be calculated for both imidazole nitrogen atoms, as is shown in Figure 9. The distribution around the N3 nitrogen atom shows a clear if weak hydrogen-bond interaction, while there is no such peak in the $g_{NO}(r)$ for the N1 position. These distributions can also be compared to similar radial distribution functions for water oxygen atoms around these nitrogen atoms, as shown in Figure 10. As can be seen, the sugar hydroxyl oxygen atoms are hydrogen bonding to these two atoms in the same manner as do the water molecules. Table 3 lists the number of hydrogen bonds to water and to collectively any sugar oxygen atom calculated from the trajectory using as a definition a distance cutoff of 3.4 Å and an angle cutoff of 150˚ or greater. The unprotonated N3 atom makes, on average, approximately 1.4 hydrogen bonds to water, and approximately 0.2 to a sugar hydroxyl group, so that this atom is generally making a little under two hydrogen bonds. The near absence of hydrogen bonding for the N–H group of N1 is due to the very low charges of these atoms, since the polarity of this group is insufficient to compete for partners with the much stronger water–water hydrogen bonds.

Table 3 The number of hydrogen bonds made by the imidazole nitrogen atoms to both water and glucose hydroxyl groups.

atom	hydrogen bonds to glucose	hydrogen bonds to water
N1	0.022	0.144
N3	0.214	1.393

Conclusions

The present simulations find that in aqueous solution there is a significant tendency for glucose to associate with imidazole both through face-to-face stacking and through hydrogen bonding between the glucose hydroxyl groups and the imidazole N3 atom. Both types of interactions could potentially play a role in the affinity of glucose for protein binding sites, although the magnitude of the "binding" is quite small, less than kT at room temperature, and by itself would not suffice to position an osmolyte like glucose into a protein site. Somewhat surprisingly, an even greater tendency for imidazole to self-associate was observed, by face-to-face stacking, head-to-tail chain-type interactions, and much more commonly, by edge-on "T"-type interactions. These latter two associations are presumably due to favorable electrostatic interactions, whereas the face-to-face interactions both between imidazole molecules, and between imidazole and glucose, are probably driven by hydrophobic pairing due to the weak hydration of these surfaces. Understanding such interactions could prove useful in designing improvements in binding site energetics in practical systems like cellulases, where better enzymes are needed for biomass conversion applications.

Acknowledgements

The authors thank P.E. Mason and U. Schnupf for helpful discussions. Dr. Mason also prepared Figure 1. This project was supported by the National Institutes of Health (GM63018)

and by the DOE Office of Science, Office of Biological and Environmental Research through the BioEnergy Science Center (BESC), a DOE Bioenergy Research Center.

References

(1) Delbaere, L. T. J.; Vandonselaar, M.; Prasad, L.; Quail, J. W.; Nikrad, P. V.; Pearlstone, J. R.; Carpenter, M. R.; Smillie, L. B.; Spohr, U.; Lemieux, R. U. *Trans. Am. Crystallogr. Assoc.* **1989**, *25*, 65-76.

(2) Einspahr, H.; Parks, E. H.; Suguna, K.; Subramanian, E.; Suddath, F. L. *J. Biol. Chem.* **1986**, *261*, 16518-16527.

(3) Frankel, A. E.; Burbage, C.; Fu, T.; Tagge, E.; Chandler, J.; Willingham, M. C. *Biochemistry* **1996**, *35*, 14749-14756.

(4) Quiocho, F. A. *Pure Appl. Chem.* **1989**, *61*, 1293-1306.

(5) Quiocho, F. A.; Vyas, N. K.; Spurlino, J. C. *Trans. Am. Crystallogr. Assoc.* **1991**, *25*, 23-35.

(6) Quiocho, F. A.; Vyas, K. K. *Nature* **1984**, *310*, 381-386.

(7) Kraulis, P. J.; Clore, G. M.; Nilges, M.; Jones, T. A.; Pettersson, G.; Knowles, J.; Gronenborn, A. M. *Biochemistry* **1989**, *28*, 7241-7257.

(8) Alahuhta, M.; Xu, Q.; Bomble, Y. J.; Adney, W. S.; Ding, S.-Y.; Himmel, M. E.; Lunin, V. V. *J. Mol. Biol.* **2010**, *402*, 374-387.

(9) Himmel, M. E.; Ding, S.-Y.; Johnson, D. K.; Adney, W. S.; Nimlos, M. R.; Brady, J. W.; Foust, T. D. *Science* **2007**, *315*, 804-807.

(10) Lis, H.; Sharon, N. *Curr. Opin. Struct. Biol.* **1991**, *1*, 741-749.

(11) Cuneo, M. J.; Changela, A.; Warren, J. J.; Beese, L. S.; Hellinga, H. W. *J. Mol. Biol.* **2006**, *362*, 259-270.

(12) Parsiegla, G.; Reverbel, C.; Tardif, C.; Driguez, H.; Haser, R. *J. Microbiol.* **2008**, *375*, 499-510.

(13) Mason, P. E.; Lerbret, A.; Saboungi, M.-L.; Neilson, G. W.; Dempsey, C. E.; Brady, J. W. *Proteins* **2011**, *79*, 2224-2232.

(14) Laughrey, Z. R.; Kiehna, S. E.; Riemen, A. J.; Waters, M. L. *J. Am. Chem. Soc.* **2008**, *130*, 14625-14633.

(15) Vanommeslaeghe, K.; Hatcher, E.; Acharya, C.; Kundu, S.; Zhong, S.; Shim, J.; Darian, E.; Guvench, O.; Lopes, P.; Vorobyov, I.; MacKerell, A. D. *J. Comput. Chem.* **2010**, *31*, 671–690.

(16) Tavagnacco, L.; Mason, P. E.; Schnupf, U.; Pitici, F.; Zhong, L.; Himmel, M. E.; Crowley, M.; Cesàro, A.; Brady, J. W. *Carbohydr. Res.* **2011**, *346*, 839-846.

(17) Tavagnacco, L.; Schnupf, U.; Mason, P. E.; Saboungi, M.-L.; Cesàro, A.; Brady, J. W. *J. Phys. Chem. B* **2011**, *115*, 10957-10966.

(18) Jorgensen, W. L.; Chandrasekhar, J.; Madura, J. D.; Impey, R. W.; Klein, M. L. *J. Chem. Phys.* **1983**, *79*, 926-935.

(19) Wohlert, J.; Schnupf, U.; Brady, J. W. *J. Chem. Phys.* **2010**, *133*, 155103.

(20) Brooks, B. R.; Bruccoleri, R. E.; Olafson, B. D.; Swaminathan, S.; Karplus, M. *J. Comput. Chem.* **1983**, *4*, 187-217.

(21) Brooks, B. R.; Brooks, C. L.; A.D. MacKerell, J.; Nilsson, L.; Petrella, R. J.; Roux, B.; Won, Y.; Archontis, G.; Bartels, C.; Boresch, S.; Caflisch, A.; Caves, L.; Cui, Q.; Dinner, A. R.; Feig, M.; Fischer, S.; Gao, J.; Hodoscek, M.; Im, W.; Kuczera, K.; Lazaridis, T.; Ma, J.; Ovchinnikov, V.; Paci, E.; Pastor, R. W.; Post, C. B.; Pu, J. Z.; Schaefer, M.; Tidor, B.; Venable, R. M.; Woodcock, H. L.; Wu, X.; Yang, W.; York, D. M.; Karplus, M. *J. Comput. Chem.* **2009**, *30*, 1545-1614.

(22) Guvench, O.; Greene, S. N.; Kamath, G.; Brady, J. W.; Venable, R. M.; Pastor, R. W.; Mackerell, A. D. *J. Comput. Chem.* **2008**, *29*, 2543-2564.

(23) Miyamoto, S.; Kollman, P. A. *J. Comput. Chem.* **1992**, *13*, 952-962.

(24) van Gunsteren, W. F.; Berendsen, H. J. C. *Mol. Phys.* **1977**, *34*, 1311-1327.

(25) Darden, T.; York, D.; Pedersen, L. *J. Chem. Phys.* **1993**, *98*, 10089-10092.

(26) Humphrey, W.; Dalke, A.; Schulten, K. *J. Mol. Graphics* **1996**, *14*, 33-38.

(27) Shallenberger, R. S. *Advanced Sugar Chemistry: Principles of Sugar Stereochemistry*; AVI Publishing Company, Inc.: Westport, Connecticut, **1982**.

(28) Domanska, U.; Kozlowska, M. K.; Rogalski, M. *J. Chem. Eng. Data* **2002**, *47*, 456-466.

(29) Liem, S. Y.; Shaik, M. S.; Popelier, P. L. A. *J. Phys. Chem. B* **2011**, *115*, 11389-11398.

(30) Singh, G.; Brovchenko, I.; Oleinkova, A.; Winter, R. *Biophys. J.* **2008**, *95*, 3208-3221.

(31) Mason, P. E.; Neilson, G. W.; Enderby, J. E.; Saboungi, M.-L.; Dempsey, C. E.; MacKerell, A. D.; Brady, J. W. *J. Am. Chem. Soc.* **2004**, *126*, 11462-11470.

Figure Captions

Figure 1 The binding site of a glucose binding protein (GBP), with a glucose ligand, illustrating stacking of the sugar against a tryptophan indole group. Residues within 4.5 Å of the ligand are shown, including 5 tryptophans (shown in yellow), the imidazole groups of three histidines (shown in blue), and two acid residues.[11]

Figure 2 The active site of the Cel48F enzyme from *Clostridium cellulolyticum*,[12] illustrating the position of a conserved histidine residue His 36 in the active site and the catalytic acid residue Glu 55.

Figure 3 The entrance of the active site tunnel in the cellulase Cel48F from *Clostridium cellulolyticum*, showing the location in purple of a histidine residue (His 200) which might potentially interact with or attract a cellulose chain.

Figure 4 The structure of imidazole and the atomic nomenclature used in the present study.

Figure 5 Isocontour density surfaces enclosing those regions of space, relative to a frame fixed with respect to the imidazole solute, where the density of other imidazole ring atoms exceeds 3 times the bulk value.

Figure 6 "Snapshots" take from the trajectory illustrating the relative geometries for typical imidazole interactions. Left, a T-type interaction; middle, a stacked arrangement mediated by a second T-type association; right, a chain-type geometry.

Figure 7 Isocontour density surfaces enclosing those regions of space, relative to a frame fixed with respect to the imidazole solute, where the density for the βD-glucopyranose atoms exceeds the bulk value by a factor of 2.5. Red: the density of the aliphatic protons H2 and H4; yellow: the density of the H1, H3, and H5 aliphatic protons; metallic blue: the density of the ring carbon atoms.

Figure 8 The density of βD-glucopyranose density around imidazole. Red: the density of O1, O2, O3, and O4 atoms contoured at 3x bulk density; yellow: the density of O5 atoms contoured at 3x bulk density; green: the density of O6 atoms contoured at 3x bulk density. Note particularly the density of the O5 ring atom, which illustrates the ring stacking above and below the imidazole plane.

Figure 9 The radial distribution functions for sugar oxygen atoms around the two nitrogen atoms of imidazole.

Figure 10 The radial distribution functions for sugar oxygen atoms around the two nitrogen atoms of imidazole.

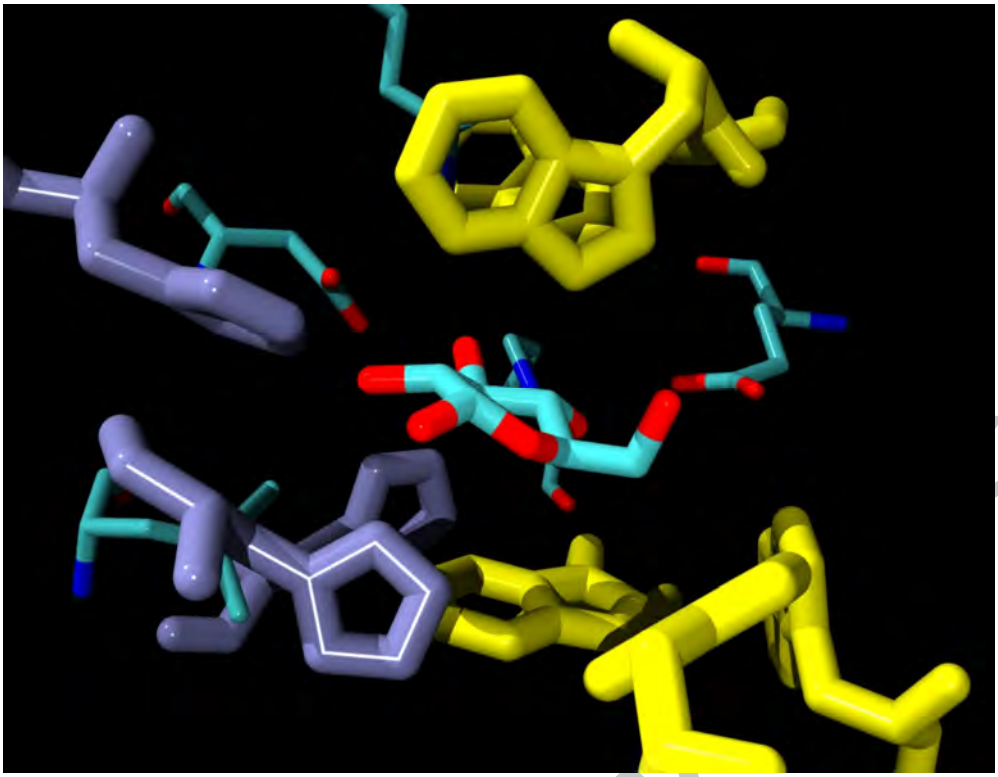

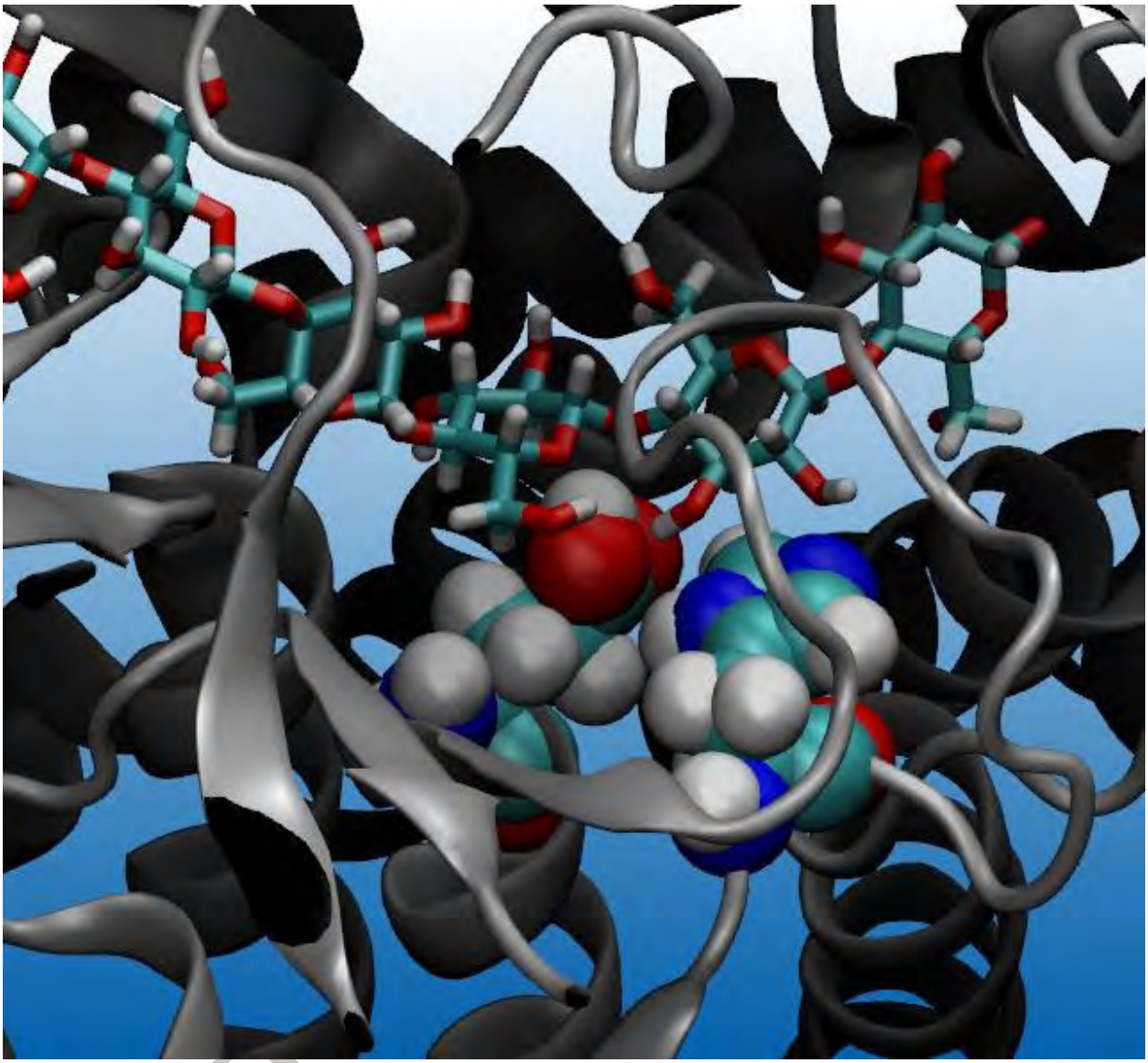

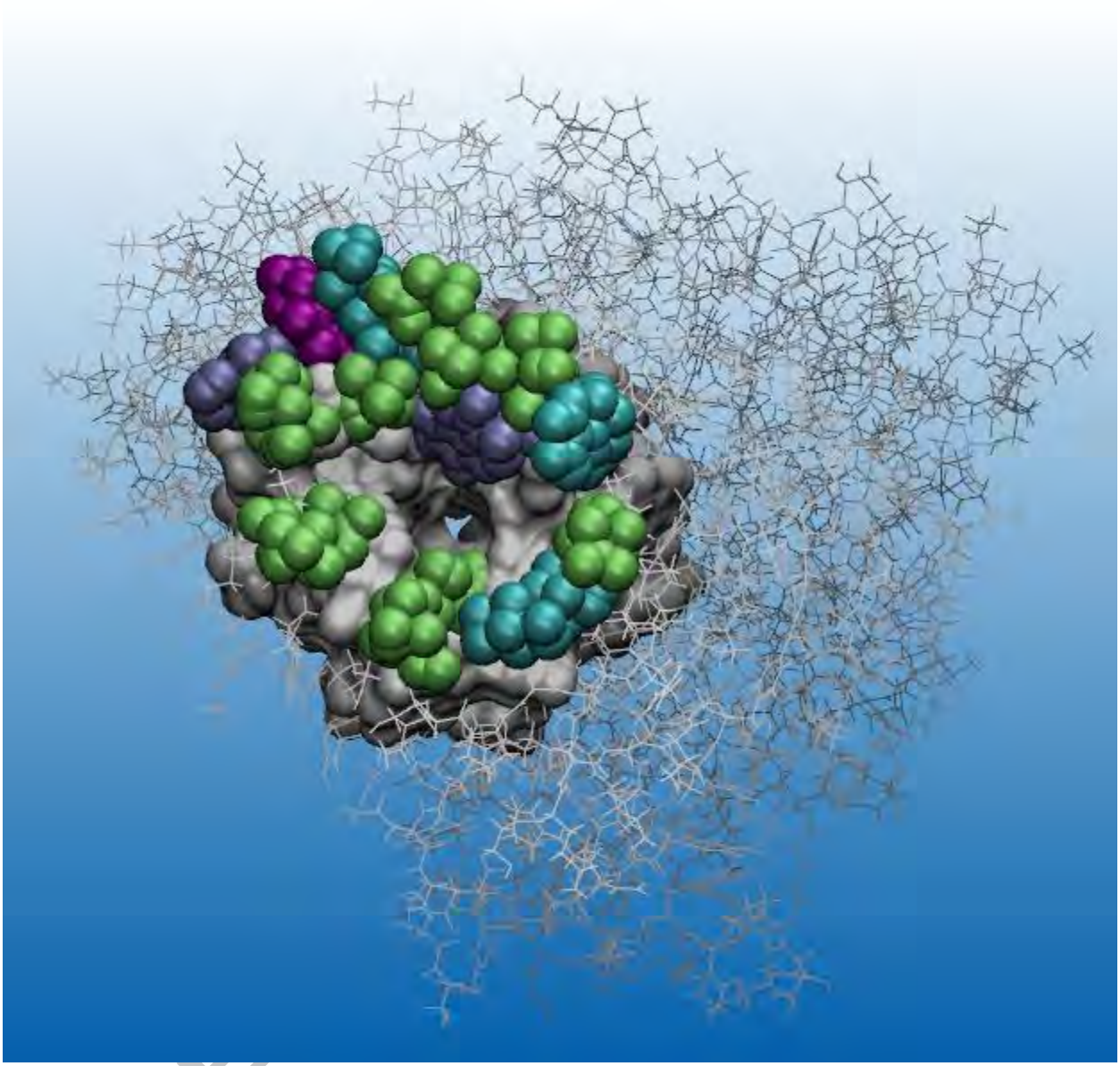

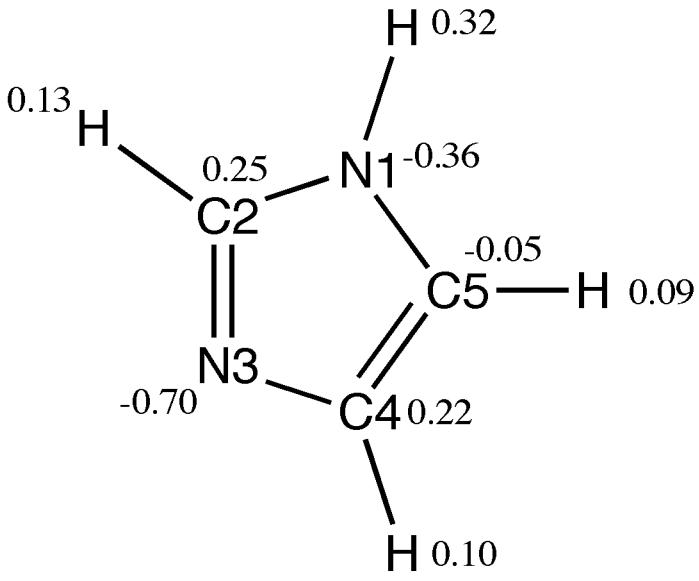

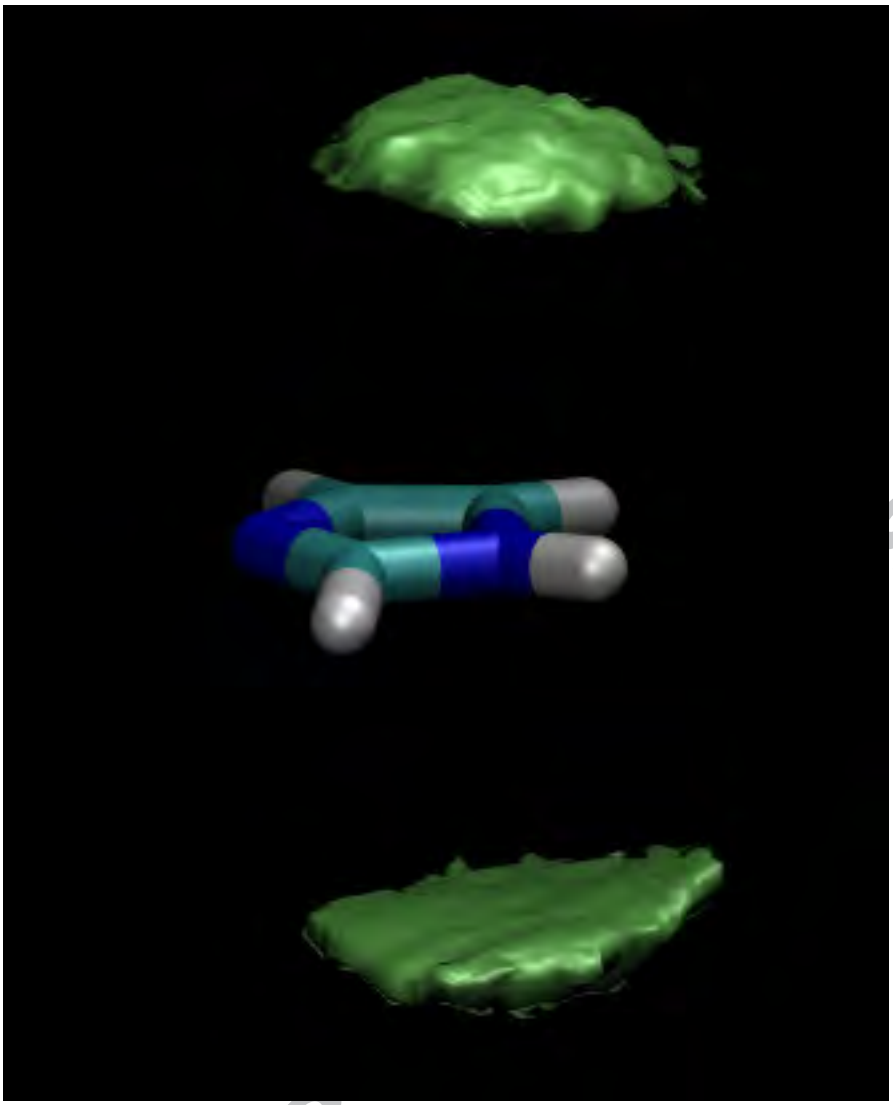

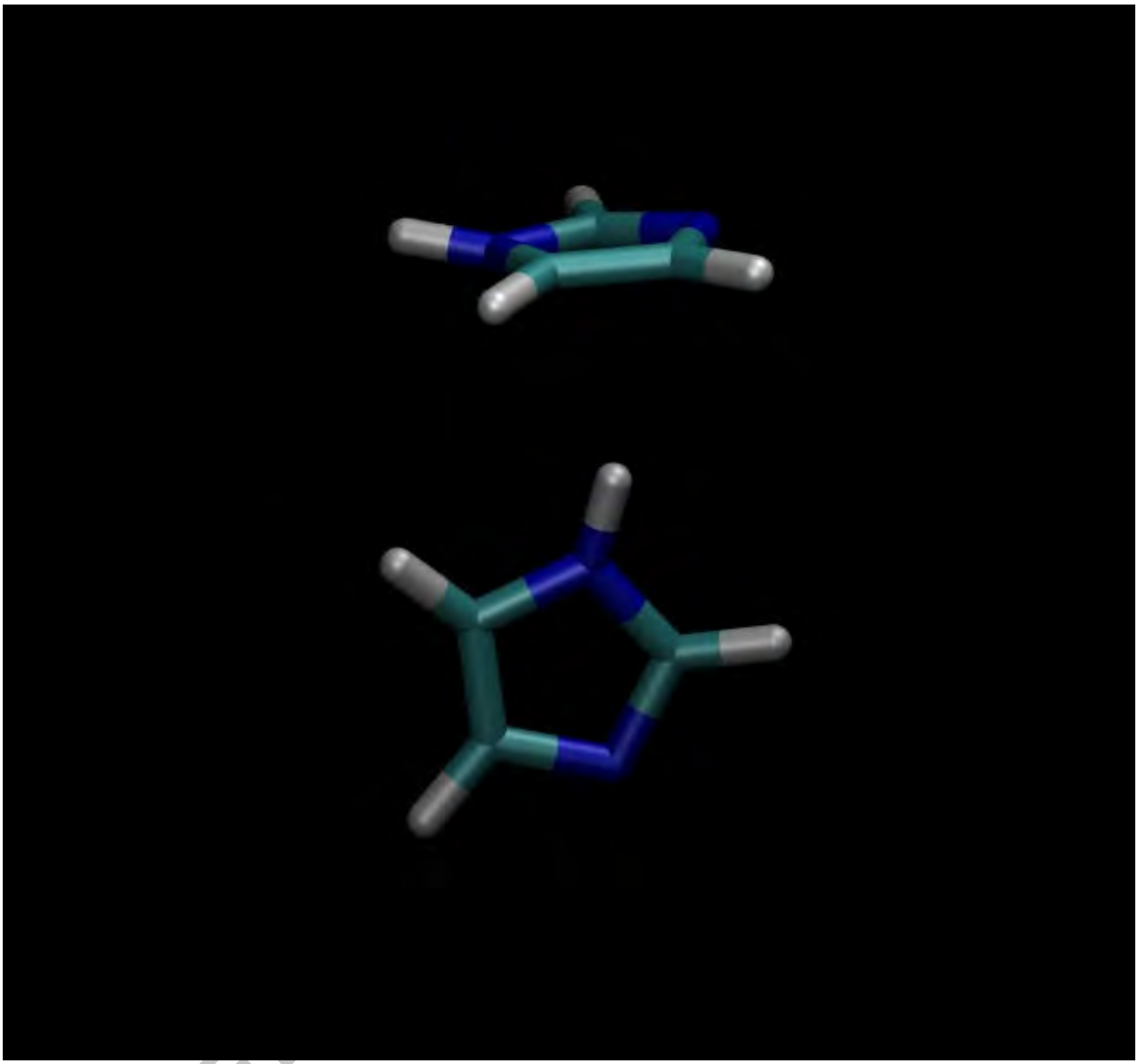

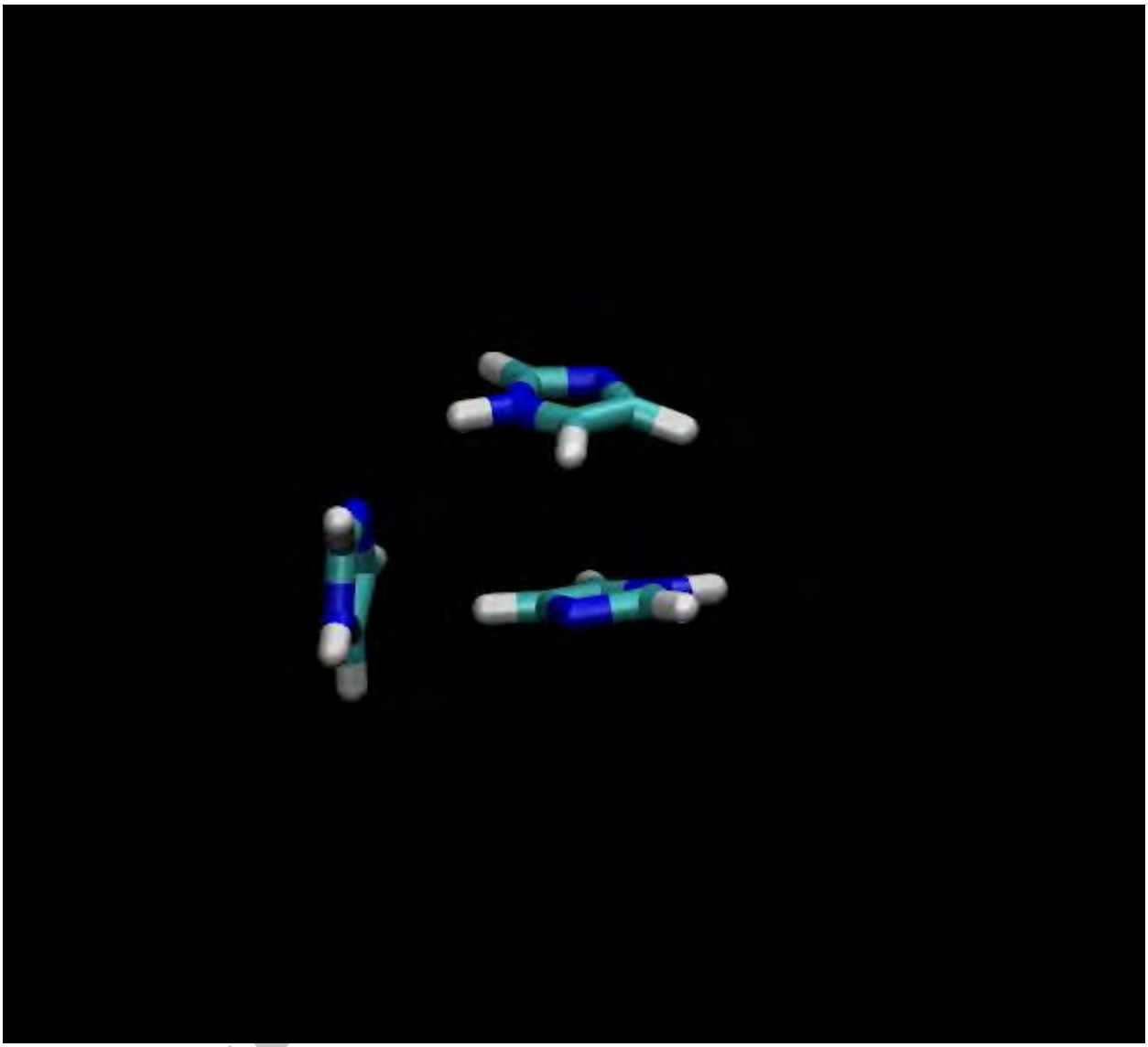

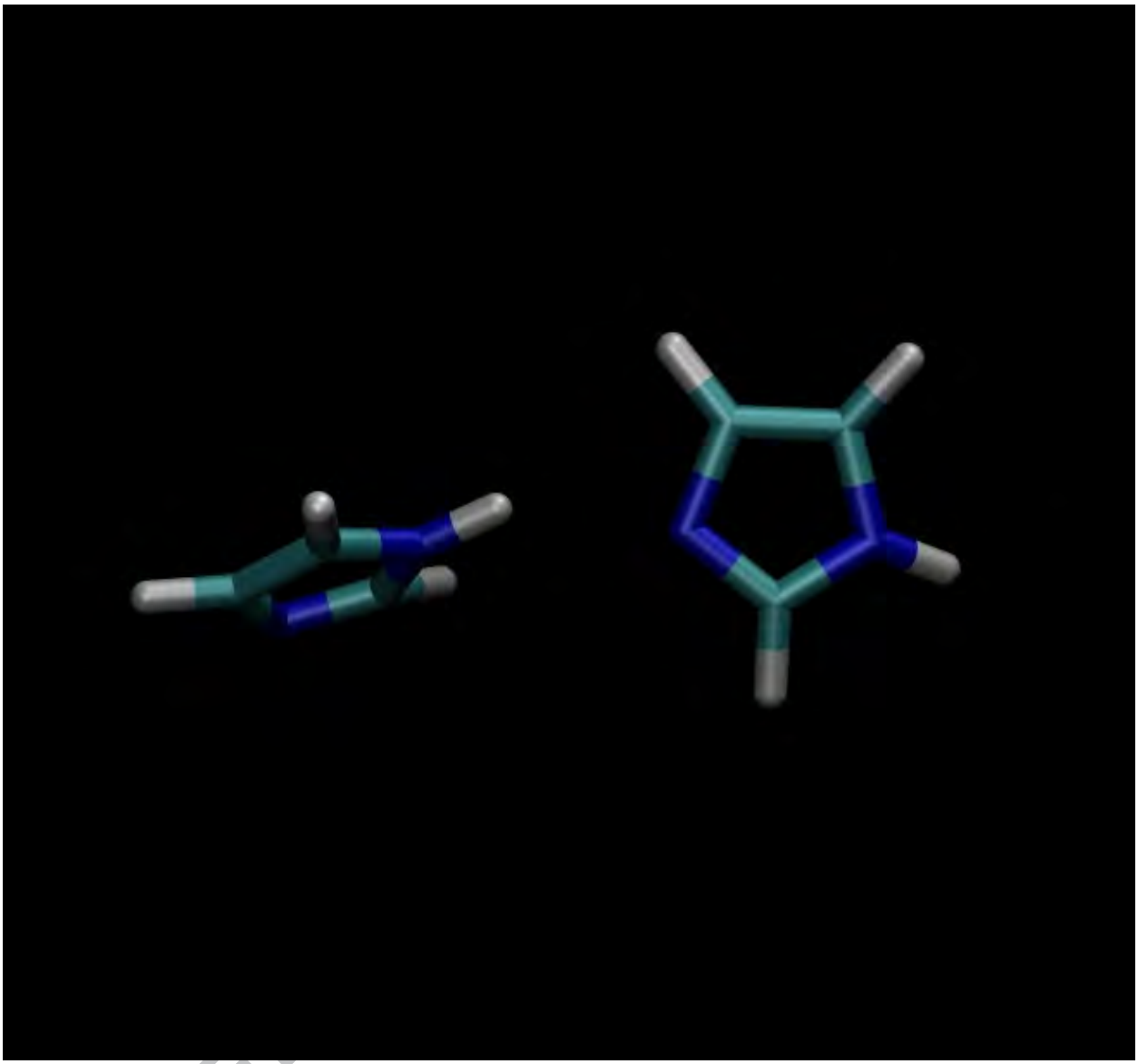

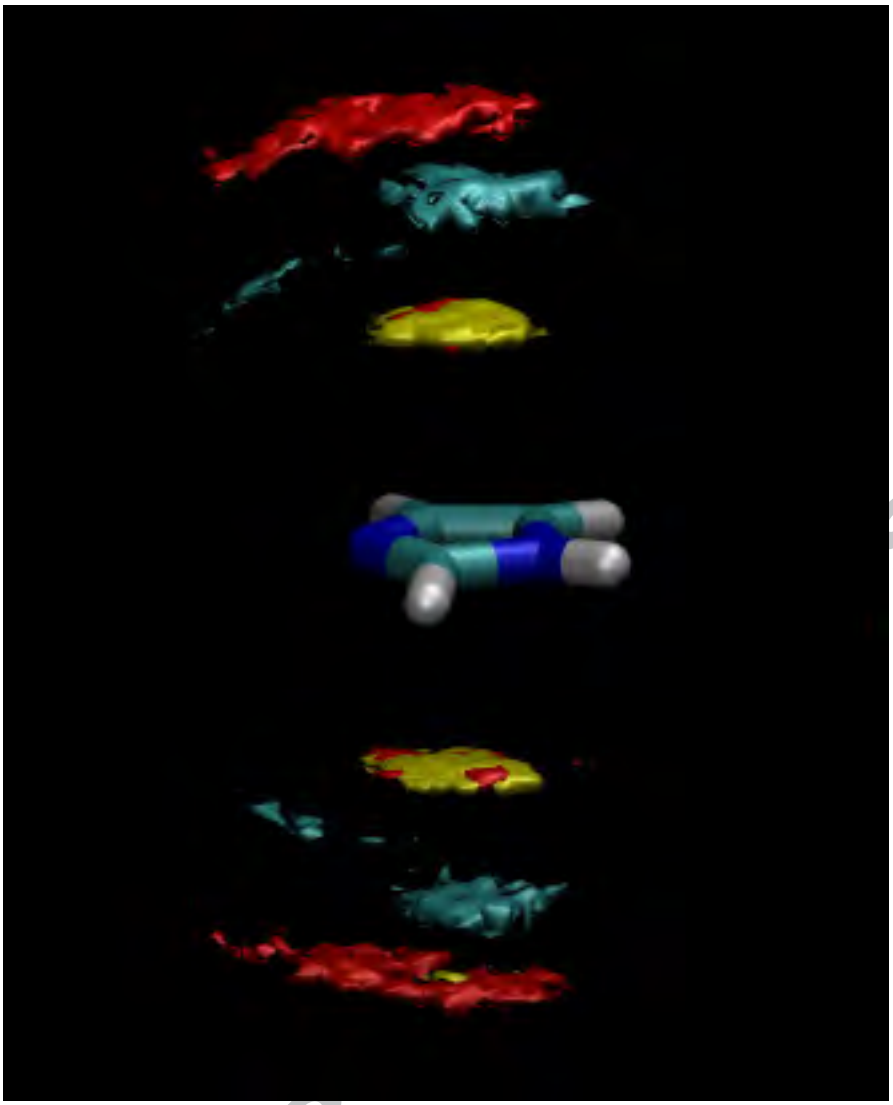

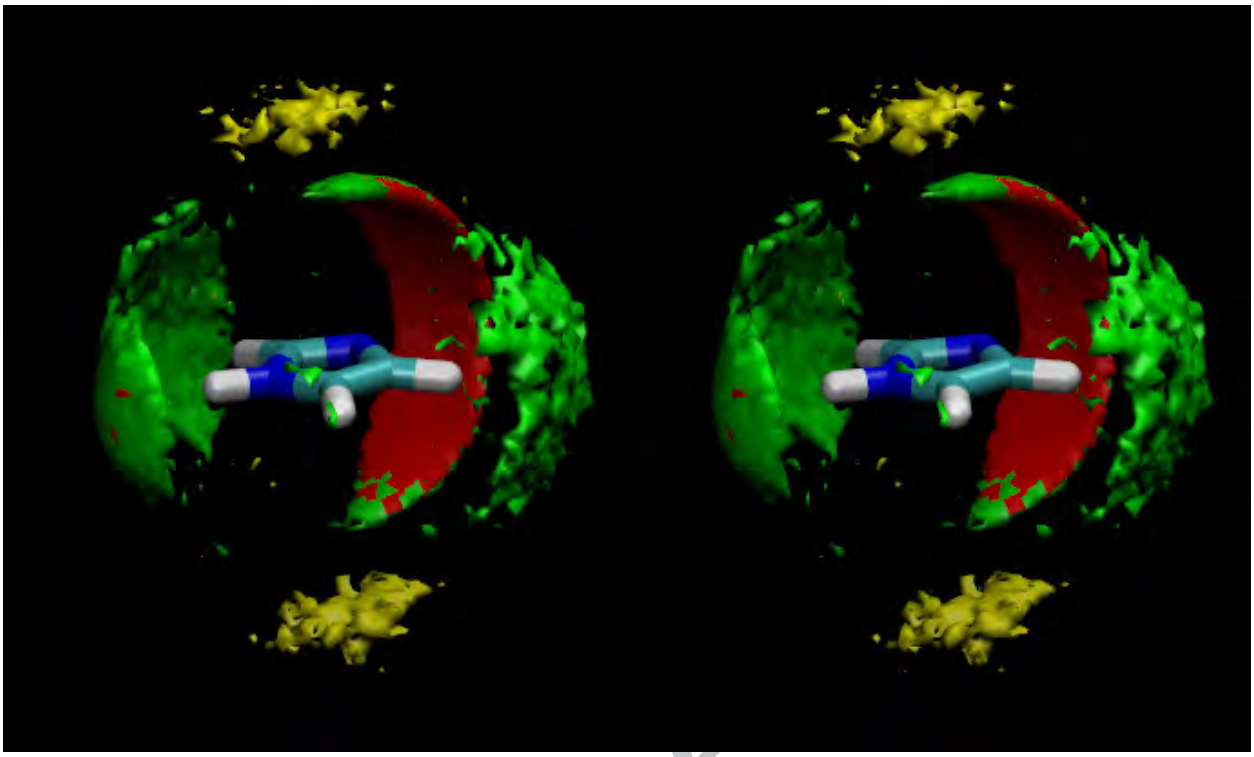

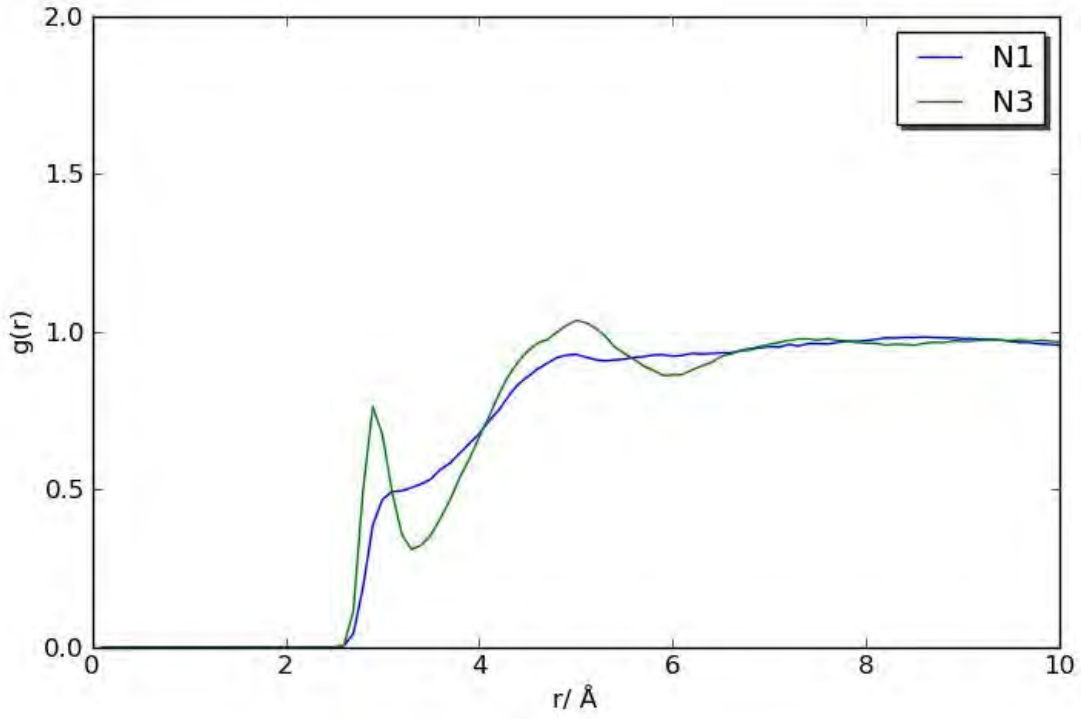

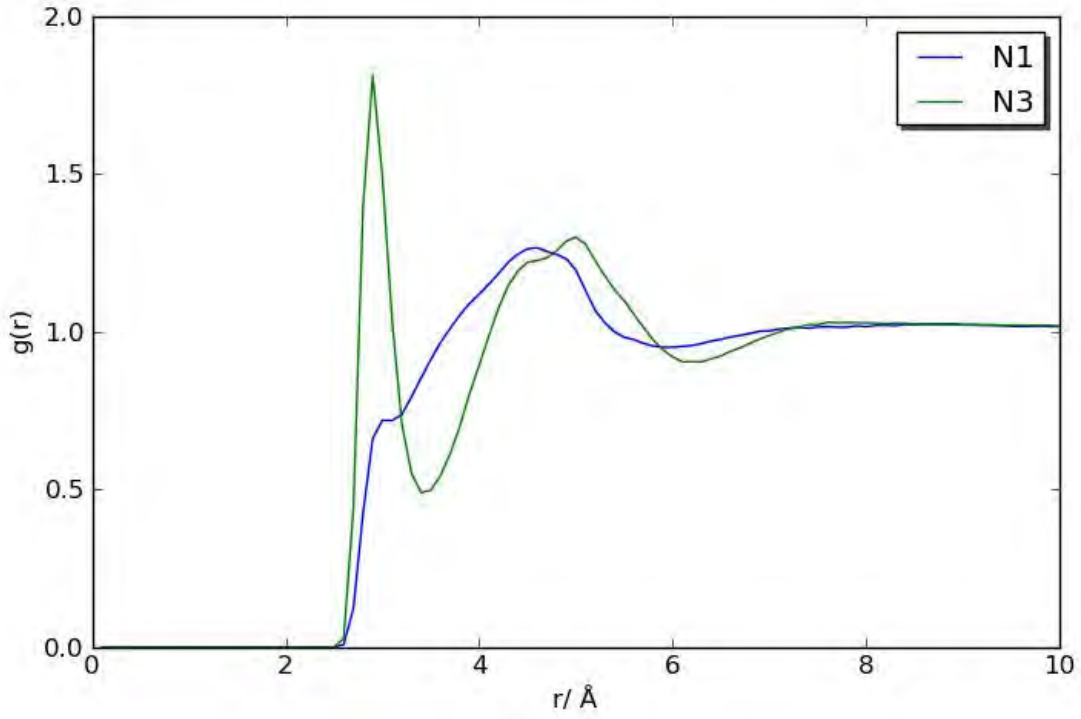

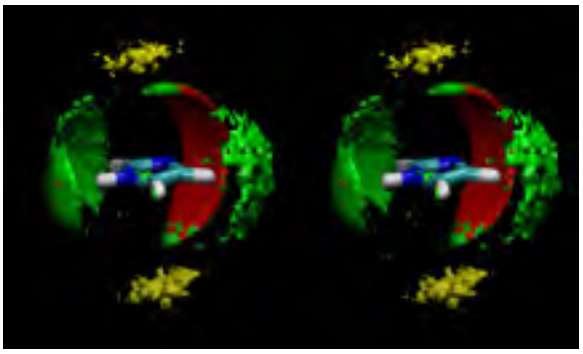

- Glucose stacks against the faces of imidazole with binding energy of ~0.5 kcal/mol
- Imidazole molecules bind to one another with a binding energy of ~0.8 kcal/mol
- Both types of binding are due to unfavorable interactions with solvent water
- However, imidazole is too small to hydrate as an extended hydrophobic surface